Astron. Astrophys. 318, 215–230 (1997)

ASTRONOMY
AND
ASTROPHYSICS

Coronae on solar-like stars

Jürgen H.M.M. Schmitt

Max-Planck-Institut für Extraterrestrische Physik, Postfach 1603, D-85740 Garching, Germany

Received 14 March 1996 / Accepted 27 June 1996

Abstract. The results of a complete and sensitive X-ray survey of all known stars of spectral type A, F, and G in the immediate solar vicinity with distances less than 13 pc are presented. The X-ray data were obtained primarily from the ROSAT all-sky survey (RASS); those program stars not detected in the RASS data, were subsequently studied in the ROSAT pointed observation program. The detection rate among the F stars in the sample is 95 %, that of the G stars 83 %, the non-detections being due to survey observations. On the other hand, none of the A-stars with spectral type earlier than A7 could be detected even in sensitive pointings. I conclude from this that coronal formation in stars with surface convection zones is universal. The X-ray luminosities range over about four orders of magnitude, and can be well described with a log-normal distribution. Large X-ray outputs are correlated with kinematic age as assessed from space motions. I show the existence of a correlation between the total emitted X-ray surface flux and spectral hardness, such that more luminous objects tend to have larger spectral hardness, thus implying higher coronal temperatures. The mean X-ray surface fluxes span the same range as is observed for various solar coronal features, with a rather well-defined minimum X-ray flux being present; this minimum X-ray surface flux agrees very well with the X-ray surface flux of solar coronal holes. It therefore appears that a coronal hole represents the minimum state of "activity" not only for the Sun but also for other stars. I discuss a few implications of this finding especially with regard to properties of stars in Maunder minima states.

Key words: stars: X-rays – coronae – nearby stars

1. Introduction

The existence of a tenuous corona around the Sun has been known for more than one hundred years. Through identification of forbidden lines detected at optical wavelengths it was realized (cf., Grottian 1939) that the temperature of the coronal gas exceeds 10^6 K, thus giving rise to the still unsolved coronal heating problem. Plasma at temperatures of a few million degrees loses the bulk of its radiative energy at soft X-ray wavelengths, and hence X-ray studies of the solar corona have become a vital tool for coronal and solar physics in general. In particular, at X-ray wavelengths the solar corona can be readily imaged with modern solar X-ray telescopes from disk center out to a few solar radii, while optical studies utilizing forbidden lines are usually restricted to regions near the solar limb.

In the context of the solar-stellar connection, one naturally expects other stars also to be surrounded by coronae. Stellar observations, however, do not permit the luxury of angular resolution, and all attempts to detect forbidden coronal lines at optical wavelengths have failed (Wallerstein et al. 1991). In the last couple of years an increasing number of radio detections of active stellar coronae has been reported (cf., Güdel 1994), but it is fair to say that stellar coronae at large can – at least at present – only be detected and studied at X-ray wavelengths. While the first generation of non-imaging X-ray missions was not sensitive enough to detect emission even from the nearest stars, the advent of imaging soft X-ray telescopes on board the *Einstein Observatory* (launched in 1978), *EXOSAT* (launched in 1983), and ROSAT (launched in 1990) allowed the study of stellar coronae at large. The first break-through in stellar X-ray astronomy was accomplished with the help of the *Einstein Observatory* (cf., Vaiana et al. 1981; Rosner, Golub and Vaiana 1985; Vaiana et al. 1992) by giving hundreds of examples of X-ray emission from almost all classes of stars. The ROSAT all-sky survey (RASS) has produced complete and unbiased samples of X-ray sources of all source classes: approximately one third of its $\approx 80\,000$ sources are of coronal origin, thus providing the largest sample of coronal X-ray emitters known to date. However, as pointed out by Schmitt et al. (1995), solar-like coronal X-ray sources – at least from the point of view of energetics – can only be detected in the close vicinity of the Sun: For a star with a soft X-ray luminosity of $2\ 10^{27}$ erg/sec, a typical value for the Sun under maximum conditions, one readily calculates a maximal distance of 9 pc, at which it can still be detected as a RASS source, given a characteristic limiting RASS X-ray flux of $2\ 10^{-13}$ erg/cm^2/sec. Under solar minimum conditions, the characteristic solar soft X-ray flux is reduced at least by one order of magnitude, emphasizing my point that stars emitting

Send offprint requests to: J.H.M.M. Schmitt, e-mail: jhs@rosat.mpe-garching.mpg.de

at solar levels or even below can be studied only if they are sufficiently close. There is considerable interest in the question whether and to what extent phenomena observed in the solar corona also occur on other stars. After all, within the context of solar physics one can deal with only one star, while in the stellar context one can study the coronal properties of stars with different ages, masses, radii, rotation rates etc. in comparison to what is known from the Sun. However, to this end the full range of stellar X-ray emission must be observed, but X-ray selected stellar samples are by necessity biased towards the intrinsically luminous X-ray emitters. Therefore the question to what extent we can consider the Sun as a typical star from the coronal point of view, cannot be satisfactorily answered with previously existing data.

Nearby solar-like stars have been systematically studied with the *Einstein Observatory*. Specifically, Maggio et al. (1987) studied all late F and G dwarf stars within a volume of 25 pc and observed with the *Einstein Observatory*, in order to assess the X-ray properties of solar-like "normal stars", and Schmitt et al. (1985) studied the X-ray properties of stars with shallow convection zones in the color range $0.1 <$ B-V < 0.5 and again within a distance of 25 pc, in an effort to investigate whether the onset of significant surface convection zones manifests itself in a detectable change of the coronal properties of these stars. Both of these studies were incomplete in the sense that by necessity they had to be restricted to those stars which were actually observed by the *Einstein Observatory* as a target or serendipitously; further, the sensitivity of these *Einstein* observations fell only occasionally below 10^{27} erg/sec, with a more typical value being $\approx 10^{28}$ erg/sec. Specifically, only 18 stars out of the sample of 61 objects studied by Maggio et al. (1987) are included in our 13 pc sample; all of these 18 stars except one were detected by ROSAT, while seven could not be detected with the *Einstein Observatory*. For the somewhat hotter stars studied by Schmitt et al. (1985) the improvement of the new ROSAT data is less significant. The sample in this paper has eight objects in common with the sample of shallow convection zone stars discussed by Schmitt et al. (1985). Seven of these eight objects were detected already with the *Einstein Observatory* and are now confirmed by ROSAT, ι Peg (= HR 8430 = Gl 848) was added to the list of known X-ray sources. I do wish to point out, however, that some of my upper limits for A-type stars are significantly below those obtained from the *Einstein* data.

Considering the fact that the solar soft X-ray luminosity is typically in the range $\approx 5\ 10^{26}$ to $\approx 2\ 10^{27}$ erg/sec, a study of stars exhibiting solar-like levels of activity is quite difficult with the *Einstein Observatory* data. As a consequence, it is next to impossible to decide on the basis of pre-ROSAT data to what extent other stars really represent solar analogs. Specifically, from the *Einstein* observations it is clear that about one third of the G stars emit at levels below 10^{27} erg/sec, but it is not clear whether there is any minimally attained X-ray luminosity and one cannot assess whether there are any X-ray dark solar-like stars.

Using new ROSAT observations, the difficulties of previous studies can be overcome, and the purpose of this paper is to present an X-ray study of a **complete volume-limited** sample of nearby stars of spectral type A, F and G. I primarily use data obtained during the ROSAT all-sky survey; those stars not detected in the all-sky survey, were systematically studied in the ROSAT pointing program. With this observing strategy I can improve on the *Einstein* observations in two important respects: First, completeness is guaranteed through the use of RASS data, and second, the required sensitivity is obtained through ROSAT pointings on those objects where deeper exposure time was needed.

The structure of this paper is as follows: In Sect. 2 I present the sample of my program stars, the new X-ray data and their analysis. The basic results are given in Sect. 3, while in Sect. 4 I discuss the detection thresholds and sensitivity, the detection completeness of my observations, construct X-ray luminosity distribution functions, demonstrate the correlation between X-ray luminosity and spectral hardness, and consider X-ray surface fluxes as well as the relationship between coronal and kinematic properties of my sample stars. In Sect. 5 I present the interpretation of my findings as well as my conclusions, which I briefly summarize in Sect. 6.

2. Observations and data analysis

2.1. Program stars

This X-ray study is based on the known sample of stars within a distance 13 pc around the Sun as listed in the Third Catalog of Nearby Stars; I use the updated version made available to me by Jahreiss (1991; personal communication). From this catalog those dwarf stars were selected with distances less than or equal to 13 pc and with B-V colors in the range $0 \leq B - V < 0.8$, thus corresponding to a spectral type of A, F and G. Since the selection was made on B-V color, there are also four K0 type stars in the sample, i.e., Gl 309, Gl 454, Gl 635 B, and Gl 764. A volume-limited study of stars with colors in excess of $B - V = 0.8$ has been performed by Schmitt et al. (1995), while a similar study of giant stars within a distance range of 25 pc has been presented by Hünsch et al. (1996). All stars classified as white dwarfs, subdwarfs or giants have been excluded from the sample in an attempt to restrict the study to main-sequence stars only; I did, however, retain some stars classified as luminosity class IV or VI. My full sample consists out of a total of 74 stars. A number of objects are in binary systems which cannot be resolved or for which no high angular resolution X-ray data are available at present; a detailed account of these cases and how they were treated is presented in Sect. 3.2 In Table 1 I list my sample stars by their Gliese (Gl) and HD numbers, give spectral types (as given in the most recent version of this catalog), absolute and apparent magnitudes, distances (in pc), B-V colors, and U, V, W space motions (in km/sec). Obviously, the composition of my sample by spectral type represents the space densities of stars of different masses. Thus, the sample contains only five A-type stars: Sirius (= Gl 244A) of type A0V, β Leo (= Gl 448) of type A3V, Vega (= Gl 721) of type A0V, Altair (=Gl 768) of type A7 IV-V, and Fomalhaut (= Gl 881) of type A3V. In this paper I will not discuss the X-ray properties of Sirius A, which

Table 1. Solar-like stars

Name	HD number	Spectral type	M_{abs}	M_{app}	d (pc)	B-V	U km/sec	V km/sec	W km/sec
Gl 17	1581	F9 V	4.94	4.22	7.19	0.58	-60	-4	-38
Gl 19	2151	G2 IV	3.76	2.80	6.44	0.62	-51	-42	-29
Gl 34 A	4614	G3 V	4.58	3.45	5.94	0.57	-30	-11	-15
Gl 53 A	6582	G5 VI	5.81	5.17	7.43	0.69	-41	-156	-34
Gl 55	7570	F8 V	4.53	4.96	12.20	0.58	-36	-18	-11
Gl 71	10700	G8 Vp	5.77	3.49	3.50	0.72	18	28	13
	12545	G5	7.82	8.36	12.82				
Gl 92	13974	G0 Ve	4.83	4.87	10.19	0.61	-33	-46	11
Gl 95	14412	G5 V	5.87	6.34	12.42	0.73	-11	27	-10
Gl 97	14802	G1 V	4.80	5.20	12.05	0.60	-11	-13	-14
Gl 107 A	16895	F7 V	3.63	4.13	12.61	0.49	-32	0	0
Gl 124	19373	G0 V	3.88	4.05	10.82	0.60	-77	-17	22
Gl 136	20766	G2 V	5.40	5.54	10.68	0.64	-63	-42	13
Gl 137	20630	G5 Ve	4.92	4.82	9.57	0.68	-22	-4	-4
Gl 138	20807	G1 V	4.95	5.24	11.43	0.60	-66	-44	15
Gl 139	20794	G5 V	5.28	4.26	6.27	0.71	-81	-94	-27
Gl 177	30495	G1 V	4.98	5.49	12.67	0.63	-23	-9	-3
Gl 178	30652	F6 V	3.81	3.19	7.51	0.45	-26	-14	3
Gl 216 A	38393	F6 V	4.06	3.58	8.01	0.47	17	5	-10
Gl 222 AB	39587	G0 V	4.47	4.40	9.70	0.59	14	3	-9
Gl 231	43834	G5 V	5.37	5.08	8.76	0.72	17	-30	-12
Gl 244 A	48915	A1 V	1.47	-1.43	2.63	0.00	15	1	-11
Gl 280 A	61421	F5 IV-V	2.66	0.38	3.50	0.42	5	-8	-19
	68835	G5	6.84	7.32	12.50				
Gl 302	69830	G7.5 V	5.47	5.97	12.61	0.76	29	-62	-10
Gl 309	72673	K0 V	5.97	6.39	12.15	0.78	-75	5	-25
Gl 327	76151	G3 V	5.74	6.00	11.29	0.67	-32	-21	-3
Gl 356 A	82885	G8 V	5.11	5.41	11.49	0.77	-38	-17	-16
Gl 364	84117	F9 IV	4.50	4.93	12.20	0.53	-34	-28	8
Gl 395	90839	F8 V	4.30	4.84	12.82	0.52	-14	-2	2
Gl 423 A	98231	G0 Ve	4.24	4.33	10.42	0.59	-3	-33	-21
Gl 423 B	98230	G0 Ve	4.70	4.80	10.42		-3	-33	-19
Gl 434	101501	G8 Ve	5.65	5.33	8.62	0.72	7	-15	-4
Gl 442 A	102365	G5 V	4.84	4.90	10.30	0.66	-68	-40	4
Gl 448	102647	A3 V	1.63	2.14	12.67	0.09	-23	-19	-9
Gl 449	102870	F9 V	3.58	3.61	10.12	0.55	37	3	6
Gl 451 A	103095	G8 VI	6.77	6.45	8.62	0.75	265	-149	-18
Gl 454	104304	K0 IV	5.02	5.55	12.79	0.77	19	-16	-17
Gl 475	109358	G0 V	4.57	4.27	8.72	0.59	-32	-4	1
Gl 482 A	110379	F0 V	3.43	3.46	10.13	0.36	-28	-6	-18
Gl 482 B	110380	F0 V	3.49	3.52	10.13		-28	-6	-18
Gl 502	114710	G0 V	4.65	4.26	8.35	0.57	-46	10	7
Gl 506	115617	G6 V	4.99	4.74	8.92	0.71	-25	-50	-33
Gl 512.1	117176	G2.5 Va	5.23	4.98	8.93	0.71	7	-26	1
Gl 534	121370	G0 IV	2.78	2.68	9.55	0.58	8	-15	-1
Gl 534.1A	121384	G8 V	5.70	6.00	11.49	0.78	0	-8	-11
Gl 549 A	126660	F7 V	3.60	4.06	12.35	0.50	8	-28	4

Table 1. (continued)

Name	HD number	Spectral type	M_{abs}	M_{app}	d (pc)	B-V	U km/sec	V km/sec	W km/sec
Gl 559 A	128620	G2 V	4.38	0.01	1.34	0.64	-32	4	14
Gl 566 A	131156	G8 Ve	5.57	4.70	6.71	0.73	6	1	-1
Gl 575 A	133640	F9 V n	4.84	5.19	11.75	0.65	-16	-30	-15
Gl 575 B		dG2	5.61	5.96	11.75		-13	-12	13
	138441	G5	7.42	7.70	11.36				
Gl 598	141004	G0 V	4.05	4.43	11.92	0.60	-50	-25	-41
Gl 601 A	141891	F2 IV	2.41	2.84	12.18	0.29	-15	-17	-11
Gl 603	142860	F6 V	3.47	3.85	11.89	0.48	60	-36	-26
Gl 611 A	144579	G8 V	6.18	6.66	12.48	0.73	-34	-56	-22
Gl 620.1A	147513	G3/5 V	4.85	5.39	12.82	0.63	17	-3	-1
Gl 624	147584	G0 V	4.74	4.91	10.82	0.55	12	4	-6
Gl 635 A	150680	G0 IV	2.89	2.91	10.10	0.65	-54	-47	-26
Gl 635 B		K0 V	5.40	5.40	10.10				
Gl 666 A	156274	G8 V	6.13	5.53	7.58	0.77	28	19	-29
Gl 691	160691	G5 V	5.20	5.14	9.71	0.70	-12	-4	-2
Gl 695 A	161797	G5 IV	3.73	3.42	8.69	0.75	17	-33	-5
Gl 713 AB	170153	F7 V	4.18	3.57	7.54	0.49	3	39	-2
Gl 721	172167	A0 V	0.59	0.03	7.72	0.00	-15	-5	-7
Gl 764	185144	K0 V	5.93	4.68	5.61	0.79	30	44	-17
Gl 768	187642	A7 IV-V	2.29	0.77	4.98	0.22	-29	-10	-2
Gl 780	190248	G8 V	4.78	3.56	5.71	0.76	-47	-12	-13
Gl 805	197692	F5 V	3.56	4.13	12.99	0.43	23	-2	-15
Gl 827	203608	F8 V	4.53	4.22	8.66	0.49	-13	42	6
Gl 848	210027	F5 V	3.27	3.76	12.52	0.44	-16	-7	-7
Gl 853 A	211415	G1 V	4.97	5.39	12.14	0.60	-27	-37	7
Gl 881	216956	A3 V	2.09	1.16	6.51	0.09	-5	-7	-10
Gl 914 A	224930	G3 V	5.31	5.81	12.56	0.67	-10	-78	-36

is accompanied by the famous X-ray bright white dwarf Sirius B. The two stars cannot resolved in PSPC data. A ROSAT HRI pointing on the Sirius system was carried out in March 1991, at a time when the separation between the two stars was only 3 arc sec. Inspection of the image (after despeckling, cf., Schmitt et al. 1994) shows an elongation of the image along the known position angle, however, the separation is too close to derive a count rate reliable and precise enough to assess whether this rate is consistent with that expected from the known ROSAT HRI UV leak (cf., Schmitt et al. 1993). Sirius A is therefore left out from all further considerations, and my useful sample thus contains only 73 stars.

2.2. X-ray observations and data analysis

The primary data base is that provided by the ROSAT all-sky survey. A detailed description of the ROSAT satellite and its hardware is given by Trümper (1983) and Pfeffermann et al. (1986). Here it suffices to note that during the all-sky survey the ROSAT satellite was scanning the sky along great circles perpendicular to the plane of the ecliptic. By following the apparent solar motion the whole sky was covered. During a given scan, an X-ray source stayed in the 2 degree field of view of the ROSAT Position Sensitive Proportional Counter (PSPC) for up to 30 seconds; the overall survey observations thus consist of a series of individual co-added "snapshots" yielding a total useful exposure time of typically 400 - 600 seconds . For the analysis of the survey observations the same procedures as used by Schmitt et al. (1995) were employed. Program stars not detected in the all-sky survey were observed in the ROSAT pointing program. The sources were placed on-axis with typical exposure times between 1 and 2 ksec, but in some cases deeper exposures were obtained (cf., information provided in Table 2).

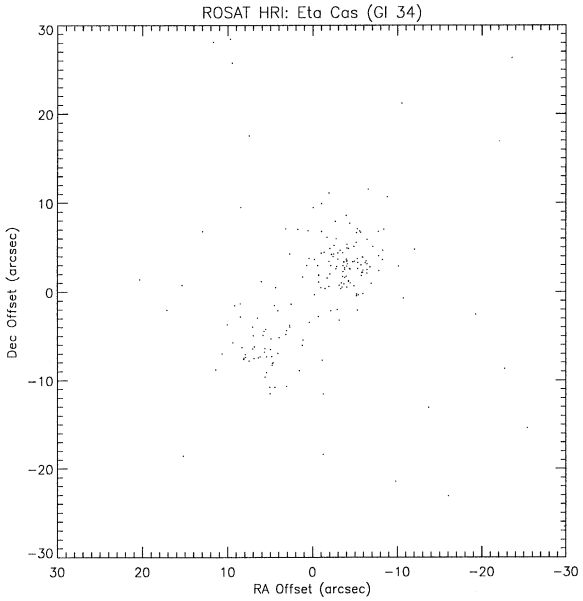

Fig. 1a. ROSAT HRI images of resolved binary systems containing nearby solar-like stars in visual double stars. All the images show the actual recorded photon events in the highest possible angular resolution (which oversamples the point response by a factor of 10) in relative coordinates. This is Gl 34 A/B; for details see text.

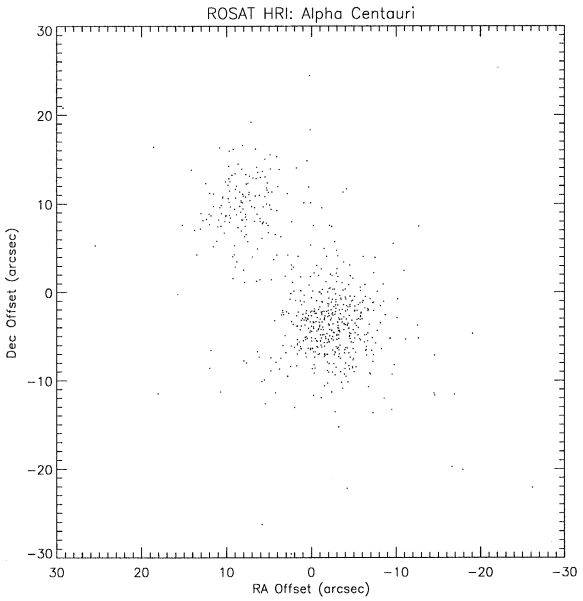

Fig. 1b. ROSAT HRI image of α Cen A/B; for details see text.

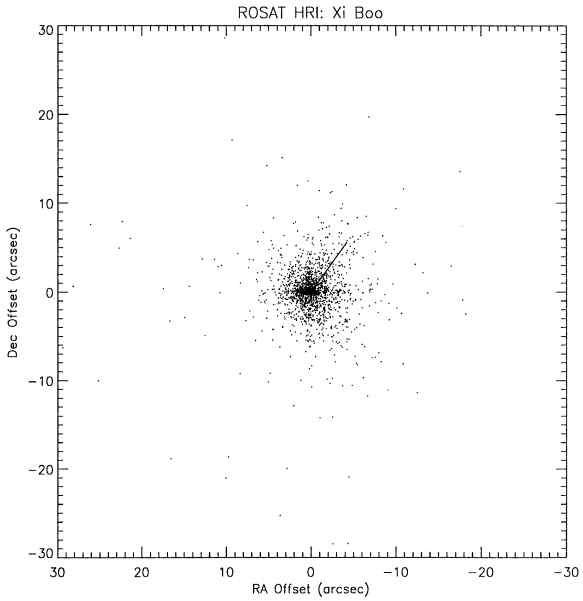

Fig. 1c. ROSAT HRI image of ξ Boo; no emission from secondary is detected, for details see text.

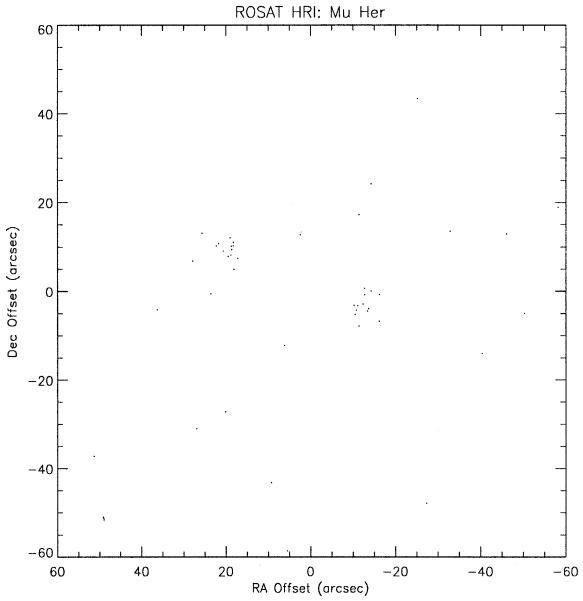

Fig. 1d. ROSAT HRI image of μ Her A/B; for details see text.

3. Results

3.1. Basic data

The basic results of our X-ray observations are presented in Table 2, where I provide the star name in column 1, the observing mode ("SU" for survey data, "PO" for pointing data, and "BO" for pointing data obtained with the boron filter) in column 2, the exposure time (in sec) in column 3. In column 4 I give an upper limit flag "UL" for those stars not detected, which remains empty for the detections. For those cases the entry in column 5 provides a 95 % confidence upper limit to the PSPC count rate in the broad band while column 7 remains empty. For the detections I give the PSPC broad band count rates and their "1 σ" errors in columns 5 and 6 of Table 2. In column 7 of Table 1 the existence likelihood (ML) of the detections is listed; it provides a measure of how much the assumption "source plus background" improves the statistical description of the data over the assumption "background only" (cf., Cruddace et al. 1988). Candidate positions, where sources with an existence likelihood < 6 have been found, I consider as upper limits. Col. 8 in Table 2 denotes the hardness ratio as determined from the PSPC data.

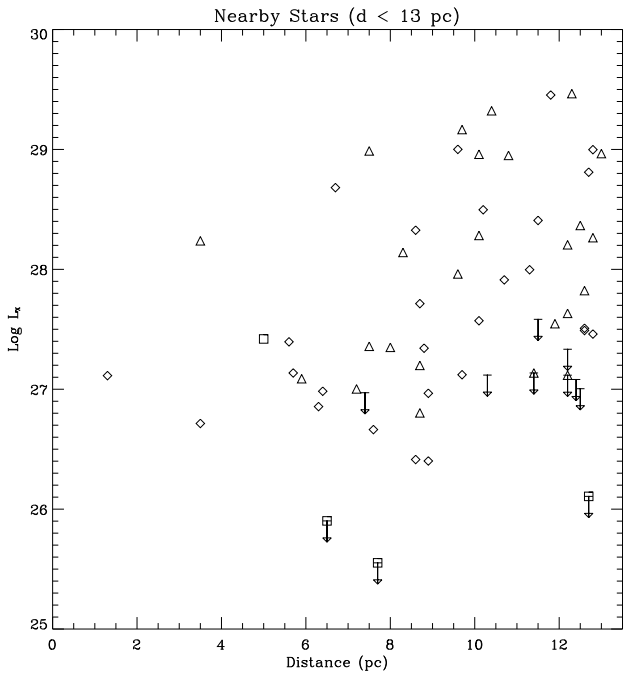

Fig. 2. Plot of X-ray luminosity L_X vs. distance d (in parsec) for our sample stars. A-type stars are drawn as squares, F-type stars as triangles, and G- and K–type stars as diamonds; upper limits are additionally indicated by downward arrows. Note that the sample is unbiased in terms of limiting X-ray luminosity with intrinsically faint stars being detected at large distances.

Denoting by H and S the counts recorded in the soft and hard PSPC pulse height channels respectively, the hardness ratio HR is defined through

$$HR = \frac{H - S}{H + S};$$

as soft band I use the PSPC pulse height channels 11 - 41, as hard band those between 52 and 201, respectively. In those cases where a significant detection was obtained only in the soft band, a hardness ratio value HR = -1 was adopted. In col. 9 of Table 1 I provide the logarithmic X-ray luminosities in the 0.1 - 2.4 keV pass band, calculated with the distances in Table 1 and a conversion factor (from count rate to energy flux) computed from the hardness ratio HR through $CEF = (5.30\ HR + 8.31)\ 10^{-12}\ erg/cm^2/count$, i.e., using the same procedure as Schmitt et al. (1995): in those cases where only soft counts (i.e., HR=-1) were recorded, a value of CEF = 6 $10^{-12}\ erg/cm^2/count$ was used. In column 10 I indicate the fraction f of the total count rate assigned to individual binary components; for single stars, f = 1 by definition. In the absence of any further information the total flux was divided equally among all system components. In those cases where HRI pointings were available I used the flux division as measured with the HRI. In the following section I discuss how the all individual cases were treated.

3.2. Notes on individual stars

In the following sections some notes on individual stars are provided. Specifically I discuss how the known binary or multiple systems were treated; in some cases ambiguities in the attribution of the X-ray emission could be resolved with new ROSAT HRI images. I also give a very brief discussion of the PSPC observation of Vega.

Gl 34 A/B (= η Cas): Consists of a G0V and M0V star, separated by $\sim$ 12 arc sec. In Fig. 1a I display a ROSAT HRI image of η Cas, clearly showing two sources. The northern source is Gl 34 B, the flux is distributed in the ratio 1: 2.25 between the A and B components, i.e., the M-star is the X-ray brighter one, consistent with *Einstein Observatory* HRI observations (cf., Harris & Johnson 1985).
Gl 53 A/B (= μ Cas): Close pair, unresolvable for the ROSAT PSPC and HRI. $\Delta m > 3$; μ Cas could not be detected in the RASS data.
HD 12545: Long-Period RS CVn star (cf., Bopp et al. 1993.
Gl 107 A/B (= θ Per): Wide pair, consisting of F7V and M1V star at 22 arc sec separation; since no ROSAT HRI observations are available, X-ray emission is equally attributed to both components.
Gl 216 A/B (= γ Lep): Wide pair, consisting of F6V and K2V star. *Einstein Observatory* HRI observations yielded a flux ratio of 1:6.6 (cf., Schmitt et al. 1985).
Gl 222 A/B (= χ^1 Ori): Wide pair consisting of G0V star and dM star. Following Haisch et al. (1994), we attribute all the X-ray emission to the G-type star.
Gl 280 A/B (= α CMi) = Procyon: Consists of F5 IV-V star and cool white dwarf; the X-ray emission comes exclusively from the non-degenerate star (cf., Schmitt et al. 1985).
Gl 356 A/B: (= 11 LMi) Faint, late-type companion at 4 arc sec distance (cf., Poveda et al. 1994). All the X-ray emission is attributed to primary.
Gl 423 A/B (= ξ UMa): Close pair, unresolvable for the ROSAT PSPC and HRI. Consists of two G0Ve stars, both of which are spectroscopic binaries. The X-ray emission is equally distributed among components.
Gl 442 A/B (= HR 4523): Very faint companion (LHS 313) 25 arc sec away (cf., Poveda et al. 1994). All the X-ray emission is attributed to primary.
Gl 451 A/B: Close pair, unresolvable for the ROSAT PSPC and HRI. Faint companion, all the X-ray emission is attributed to primary.
Gl 482 A/B: Close pair, unresolvable for the ROSAT PSPC and HRI. Consists of two almost identical F0V stars, thus X-ray emission is equally distributed among components.
Gl 534.1A (= HR 5236): Poveda et al. (1994) list faint companion 33 arc sec away. Gl 534.1A was not detected in the RASS data.
Gl 549 A/B (= θ Boo): Wide pair, consisting of G2V and late-type star more than 1 arc min away. All the X-ray emission is attributed to primary since RASS position agrees very well with primary position.
Gl 559 A/B (= α Cen): Wide pair, consisting of G2V and K0V

Table 2. X-ray data for solar-like stars

Name	Mode	Exposure sec	UL	Rate cts/sec	Error cts/sec	Likeli-hood	HR	L_X	Frac
Gl 17	PO	2426.6		2.62e-02	3.6e-03	110.3	-1.00	27.00	1.00
Gl 19	SU	393.7		3.21e-02	1.0e-02	16.9	-1.00	26.98	1.00
Gl 34 A	SU	419.8		1.13e-01	1.8e-02	85.9	-0.68	27.08	0.44
Gl 53 A	SU	246.4	<	2.01e-02		1.8	-1.00	26.97	1.00
Gl 55	SU	333.8		3.41e-02	1.2e-02	17.1	-1.00	27.63	1.00
Gl 71	SU	476.4		6.06e-02	1.3e-02	33.1	-1.00	26.71	1.00
HD 12545	SU	108.3		2.36e-01	5.4e-02	144.7	0.39	29.21	1.00
Gl 92	SU	218.1		2.86e-01	3.8e-02	207.6	-0.43	28.50	1.00
Gl 95	SU	399.5	<	1.50e-02		0.7	-1.00	27.08	1.00
Gl 97	SU	301.3		4.18e-01	4.0e-02	674.8	-0.05	29.05	1.00
Gl 107 A	SU	542.7		1.29e-01	1.7e-02	152.2	-0.70	27.82	0.50
Gl 124	SU	537.9		1.83e-02	7.2e-03	6.3	-1.00	27.10	1.00
Gl 136	SU	360.9		9.07e-02	1.9e-02	43.5	-1.00	27.91	1.00
Gl 138	SU	361.1	<	1.56e-02		0.1	-1.00	27.14	1.00
Gl 137	SU	246.7		8.90e-01	6.2e-02	1102.9	-0.32	29.00	1.00
Gl 139	PO	1793.2		2.44e-02	4.0e-03	72.2	-1.00	26.86	1.00
Gl 177	SU	540.5		3.49e-01	2.7e-02	657.6	-0.36	28.81	1.00
Gl 178	SU	410.4		1.33	5.8e-02	2880.0	-0.29	28.99	1.00
Gl 216 A	SU	501.8		2.53e-01	2.5e-02	333.2	-0.50	27.35	0.15
Gl 222 AB	SU	437.8		1.18	5.3e-02	2819.2	-0.27	29.17	1.00
Gl 231	PO	2616.0		6.73e-02	5.2e-03	499.8	-0.93	27.34	1.00
Gl 280 A	SU	437.7		3.18	8.6e-02	5428.0	-0.91	28.24	1.00
HD 68835	SU	200.2	<	1.19e-02		2.0	-1.00	27.27	1.00
Gl 302	SU	378.3		2.49e-02	9.9e-03	10.5	-1.00	27.51	1.00
Gl 309	SU	438.6	<	1.31e-02		2.4	-1.00	27.33	1.00
Gl 327	SU	354.8		8.99e-02	1.9e-02	55.7	-0.54	28.00	1.00
Gl 356 A	SU	473.9		2.26e-01	2.4e-02	253.1	-0.54	28.41	1.00
Gl 364	SU	434.7	<	1.05e-02		2.2	-1.00	27.12	1.00
Gl 395	SU	597.9		1.51e-01	1.8e-02	176.4	-0.65	28.26	1.00
Gl 423 A	SU	237.5		2.83	1.1e-01	3841.1	-0.25	29.32	0.50
Gl 423 B	SU	237.5		2.83	1.1e-01	3841.1	-0.25	29.32	0.50
Gl 434	PO	2015.9		2.72e-01	1.2e-02	3378.3	-0.42	28.33	1.00
Gl 442 A	SU	155.1	<	1.08e-02		0.4	-1.00	27.12	1.00
Gl 448	PO	15636.2	<	1.00e-03		3.2	-1.00	26.11	1.00
Gl 449	SU	414.8		2.60e-01	2.7e-02	260.6	-0.65	28.28	1.00
Gl 451 A	PO	2816.4		5.48e-03	1.7e-03	9.4	-1.00	26.41	1.00
Gl 454	SU	362.5		2.41e-02	1.1e-02	6.2	-1.00	27.46	1.00
Gl 475	PO	2665.5		4.40e-02	4.3e-03	286.9	-0.88	27.20	1.00
Gl 482 A	SU	150.0		1.10	8.9e-02	785.5	-0.13	28.96	0.50
Gl 482 B	SU	150.0		1.10	8.9e-02	785.5	-0.13	28.96	0.50
Gl 502	SU	511.6		2.85e-01	2.6e-02	323.3	-0.67	28.14	1.00
Gl 506	PO	3158.7		1.66e-02	2.4e-03	77.9	-1.00	26.97	1.00
Gl 512.1	PO	3068.6		5.67e-03	1.8e-03	6.7	-1.00	26.40	1.00
Gl 534	SU	395.7		1.15e-01	2.0e-02	54.0	-1.00	27.96	1.00
Gl 534.1A	SU	117.6	<	4.00e-02		2.0	-1.00	27.58	1.00
Gl 549 A	SU	752.7		9.16e-01	3.7e-02	4306.1	0.02	29.47	1.00

Table 2. (continued)

Name	Mode	Exposure sec	UL	Rate cts/sec	Error cts/sec	Likeli-hood	HR	L_X	Frac
Gl 559 A	PO	3273.0		4.09	1.8e-02	21729.7	-0.88	27.11	0.40
Gl 566 A	SU	405.8		1.86	7.0e-02	3640.7	-0.36	28.68	0.50
Gl 575 A	SU	882.2		2.66	5.6e-02	13037.6	-0.16	29.45	0.50
Gl 575 B	SU	882.2		2.66	5.6e-02	13037.6	-0.16	29.45	0.50
HD 138441	SU	330.2	<	1.23e-02		0.0	-1.00	27.05	1.00
Gl 598	SU	499.0		6.44e-02	1.4e-02	32.4	-1.00	27.83	1.00
Gl 601 A	SU	383.1		1.55e-01	2.2e-02	74.2	-1.00	28.20	1.00
Gl 603	SU	543.1		3.32e-02	1.1e-02	8.8	-1.00	27.55	1.00
Gl 611 A	SU	371.0	<	1.77e-02		0.9	-1.00	27.00	1.00
Gl 620.1A	SU	354.5		4.43e-01	3.7e-02	667.3	-0.25	29.00	1.00
Gl 624	SU	173.0		5.51e-01	5.8e-02	445.0	-0.26	28.95	1.00
Gl 635 A	SU	514.1		1.09e-01	1.7e-02	87.1	-0.67	27.57	0.50
Gl 635 B	SU	514.1		1.09e-01	1.7e-02	87.1	-0.67	27.57	0.50
Gl 666 A	PO	1261.2		1.16e-02	3.3e-03	16.3	-1.00	26.66	1.00
Gl 691	PO	2947.7		1.97e-02	2.7e-03	89.5	-1.00	27.12	1.00
Gl 695 A	PO	593.5		1.39e-01	1.6e-02	268.8	-0.87	27.71	1.00
Gl 713 AB	PO	3550.7		1.33e-01	6.2e-03	2020.3	-0.75	27.36	0.50
Gl 721	PO	10548.3	<	9.23e-04		1.3	-1.00	25.55	1.00
Gl 764	PO	2728.4		1.56e-01	7.7e-03	1785.6	-0.84	27.40	1.00
Gl 768	SU	494.1		1.54e-01	1.9e-02	96.1	-1.00	27.42	1.00
Gl 780	SU	132.1		3.83e-02	1.9e-02	9.0	-1.00	27.14	1.00
Gl 805	SU	324.2		3.11e-01	3.3e-02	482.1	-0.11	28.97	1.00
Gl 827	PO	1857.2		1.14e-02	2.7e-03	27.3	-1.00	26.80	1.00
Gl 848	SU	542.2		2.03e-01	2.1e-02	259.7	-0.62	28.37	1.00
Gl 853 A	SU	369.1		4.54e-02	1.3e-02	17.1	-1.00	27.35	0.50
Gl 881	BO	6207.0	<	6.60e-04		2.0	-1.00	25.90	1.00
Gl 914 A	SU	347.3		2.32e-02	1.1e-02	9.3	-1.00	27.18	0.50

star. The X-ray emission of the α Cen system was first resolved with the *Einstein Observatory* HRI (cf., Golub et al. 1981); a ROSAT HRI observation displayed in Fig. 1b confirms that the K component is brighter.

Gl 566 A/B (= ξ Boo): Wide pair, consisting of G8Ve and K4Ve star with a separation of 7 arc sec at position angle 353°. In Fig. 1c I display a ROSAT HRI image of the ξ Boo system; the observations were despeckled in a manner very similar to that described and applied by Schmitt et al. (1994) in their analysis of the Castor system. The ROSAT HRI image appears to be elongated along the (optical) position angle, however, it is also clear, that most of the emission of the ξ Boo system comes from only one component. If one interprets the emission in the vicinity of the secondary as real, the primary is also the dominant X-ray source; if only one source contributes, one cannot discriminate between the two sources. In the following I attribute all of the X-ray emission to the optical primary.

Gl 575 A/B (= 44 Boo): W UMa system.

Gl 601 A/B (= β Tra): Poveda et al. (1994) list faint companion 157 arc sec away. All the X-ray emission is attributed to primary. RASS position agrees very well with primary position.

Gl 611 A/B (= HD 144579): Poveda et al. (1994) give rather faint companion at a distance of 70 arc sec. All the X-ray emission is attributed to primary and RASS position agrees very well with primary position.

Gl 620.1A (= HR 6094): Poveda et al. (1994) list a white dwarf more than 5 arc min away. All the X-ray emission is attributed to primary.

Gl 635 A/B (= ζ Her): Close pair, unresolvable for the ROSAT PSPC and HRI. Consists of F and G star, the X-ray emission is equally distributed among components.

Gl 666A (= HR 6416): Wide pair at 10 arc sec distance, consisting of G8V and M0V star at an angular distance of 10 arc sec. PSPC pointing data is available, but only a few counts were detected. No ROSAT HRI data available, the X-ray emission is attributed to primary component.

Gl 695 A/B (= μ Her): Triple, consisting of a wide pair and a close pair, unresolvable for the ROSAT PSPC and HRI. The

two components of the close pair are M dwarfs, the other component of the wide pair is a G5IV star at a separation of 34 arc sec. The ROSAT HRI image (cf., Fig. 1 d) shows emission from both the M stars (western source) as well as the G star equally distributed among the two components.
Gl 713 A/B (= χ Dra): Close pair consisting of F and G star, unresolvable for the ROSAT PSPC and HRI. The X-ray emission is equally distributed among components.
Gl 721 (= α Lyr = Vega): An extremely weak source is found at the position of Vega; it is present only in the very softest PSPC channels, and hence completely consistent with UV contamination, which is predicted at a level of 2.2 10^{-3} cts/sec. I interpret this "detection" as upper limit.
Gl 853 A/B (= HR 8501): Poveda et al. (1994) list somewhat fainter companion 3.4 arc sec away, unresolvable for the ROSAT PSPC and HRI. X-ray emission is equally distributed among components.
Gl 914 A/B (= 85 Peg): Triple system, consisting of a close pair, unresolvable for the ROSAT PSPC and HRI, and a distant K7 component more than 1 arc min away. The X-ray emission is equally distributed among the components of close pair. The RASS position is 55 arc sec off the nominal primary position, therefore the majority for the X-ray flux might come from the late-type companion; for the moment I assign half the X-ray flux to the primary.

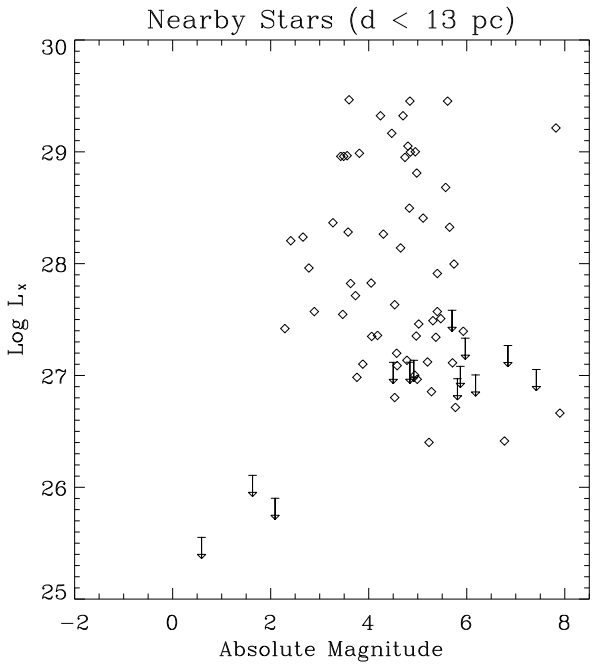

Fig. 3. Plot of X-ray luminosity L_X vs. absolute magnitude M_V for my sample stars. Detections are drawn with diamonds, upper limits by downward arrows. Note the absence of any detections for values of $M_V < 2.25$ despite the availability of extremely sensitive (pointed) observations. On the other hand, the few upper limits for stars with $M_V > 4.5$ are all due to survey data with reduced sensitivity; see text for details.

4. Discussion

4.1. Detection thresholds

The number of sources detected in an X-ray survey obviously depends on the adopted lower acceptance threshold, which is to some extent arbitrary and depends on the value of contamination through spurious sources one is willing to tolerate. As in Schmitt et al. (1995), a likelihood threshold of 6 was used as a criterion to decide between source detections and upper limits. In the likelihood range between 6 and 10 there is a total of 4 sources, i.e., Gl 124, Gl 914A, Gl 780, and Gl 454. Visual inspection of these images indeed shows the presence of sources in all these cases. I also inspected the distribution of the position offsets between X-ray source and optical star, where care was to taken to apply an appropriate proper motion correction to the actual epoch of the ROSAT observations. None of the survey detections reported here has a position offset larger than 60 arc sec, and for the pointing data the position accuracy is greatly improved. I therefore conclude that essentially all of the reported detections are real and that the sample is not contaminated by incorrectly associating "background" X-ray sources with "foreground" stars.

4.2. Survey sensitivity

The ROSAT all-sky survey is obviously a flux-limited all-sky X-ray survey. Its typical limiting flux of 2 10^{-13} $erg/cm^2/sec$ in the 0.1 - 2.4 keV pass band corresponds to a typical limiting intrinsic X-ray luminosity of $L_{X,lim} \approx 2.4\ 10^{25}\ d_{pc}^2\ erg/sec$. Thus at larger distances only the intrinsically brighter objects can be detected, and consequently in flux-limited samples one tends to find a correlation between distance and intrinsic luminosity. However, because of the pointed follow-up observations this effect is **not** present in the sample discussed in this paper. In Fig. 2 I plot X-ray luminosity L_X (or upper limits thereof) vs. distance (in pc) for my sample stars; obviously, the limiting luminosity $L_{X,lim}$ stays essentially constant throughout the sample and only for larger distances especially in the 12 - 13 pc bin the pointed follow-up observations become incomplete.

4.3. X-ray detection completeness

Inspection of Table 1 shows that 60 objects out of the total sample of 73 systems were detected as X-ray sources; if attention is restricted to stars within 12 pc, 46 out of 53 objects are detected. Among the 7 non-detections, there are 3 A-type stars (with spectral types between A0 and A3), and all of the non-detections of stars not classified as A-type are due to lower sensitivity survey data. Thus it is very suggestive to assume that lack of sensitivity is the only reason for not achieving a 100 percent detection rate for F and G type stars. On the other hand, the A-stars Vega, β Leo, and Fomalhaut remained undetected in quite deep PSPC pointings, exceeding (for Vega and β Leo) 10 ksec and resulting in rather low upper limits.

4.4. X-ray luminosity and spectral type

In Fig. 3 I plot the derived ROSAT X-ray luminosities L_X vs. absolute magnitude M_V for my sample stars. The three upper limit for stars with $M_V < 3$ correspond to the A-type stars α Lyr (A0 V), α PsA (A3V) and β Leo (A3V). The "earliest" late-type star in my sample is the A7V star Altair, already detected by the *Einstein* Observatory (cf., Schmitt et al. 1985). From Fig. 3 it is clear that X-ray emission sets in rather abruptly for stars with $M_V > 2.5$, and for F-type stars between $2.4 < M_V < 4.4$ one immediately obtains the full range of the X-ray luminosity distribution function. It is worthwhile noting that among the F-type stars the detection rate is close to 100 percent, the hottest non-detection being Gl 364 classified as F9 IV. Among the G-type stars the formal detection rate is 83 percent and hence lower. However, **all** G type stars studied in the pointed program have been detected, and hence there is no reason to assume that the non-detected stars have X-ray luminosities very much different from the detected ones. In other words, I strongly argue that the observed range of X-ray luminosities as shown in Fig. 3 is identical to the true range of X-ray luminosities of solar-like stars.

4.5. X-ray luminosity distribution functions

Next, I construct X-ray luminosity distribution functions for my sample stars using the the Kaplan-Meier product limit estimator (cf., Schmitt 1985 and references therein) for the full sample (excluding all stars classified as spectral type A), as well as the F and G star sample. Inspection of Fig. 3 shows that the X-ray luminosities of these stars are rather similar except for a slight trend for the F-type stars to be somewhat more luminous than G-type stars. In Fig. 4 I plot the overall cumulative XLDF (stepped curve) for the 13 pc sample; the position of the few upper limits is noted in the plot by small vertical bars. Also shown is the best fit log-normal distribution function (dashed smooth curve) of the form

$$p(ln(L_X)) = \frac{1}{\sqrt{2\pi}\sigma} exp(-\frac{1}{2}(\frac{lnL_X - \mu}{\sigma})^2)$$

to the data; the parameters μ and σ denote median and dispersion of the distribution function respectively. Note that for the log-normal distribution the mean of the distribution is related to the median and dispersion through

$$E(p(L_X)) = exp(\mu + \frac{\sigma^2}{2});$$

log-normal distribution function fits to X-ray selected samples of M stars from the *Einstein Medium Sensitivity Survey* have been presented by Schmitt & Snowden (1990) and for volume-complete samples of K and M stars by Schmitt et al. (1995). In Table 3 I list the fit parameters for various distribution functions, i.e, derived median, dispersion and mean values. In Fig. 5 I plot XLDFs for the stars in the color range $0.25 < B - V < 0.6$ (dashed stepped curve), $0.61 < B - V < 0.8$ (solid stepped curve) and, for comparison, the full sample (dotted stepped curve). As is obvious, the distribution function for the F-type stars lies systematically above the one for the G-type stars, with the full sample being in between. The same is true if these XLDFs are approximated by log-normal distributions (cf., Table 3); these distributions have virtually identical dispersions, and only the mean shifts towards systematically lower values.

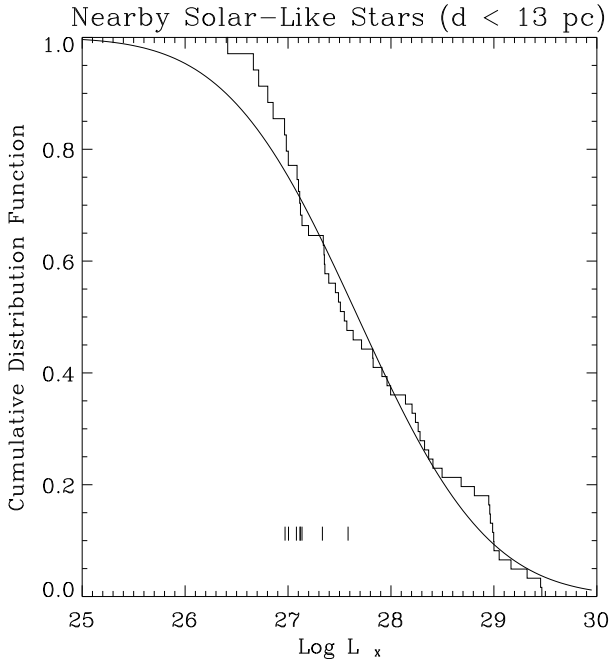

Fig. 4. Cumulative X-ray luminosity distribution function for the 13 pc sample (stepped curve) excluding the five A-type stars; the smooth line is the best log-normal distribution fit to the data, the four vertical bars indicate the positions of the non-detected stars in L_X.

Table 3. Mean X-ray properties

B-V Range	$L_{X,median}$	σ_{L_X}	Log $L_{X,mean}$
0.25 - 0.8	27.68	1.00	28.83
0.3 - 0.6	28.00	0.96	29.06
0.61 - 0.8	27.36	0.82	28.13

4.6. X-ray luminosity and kinematics

Fleming et al. (1995) showed that in their complete sample of nearby K and M dwarfs small space motions, i.e., "Young Disk" kinematics, do not necessarily lead to large X-ray luminosities, and hence called in question the use of kinematic age indicators. With the sample of F and G stars one can again check the relationship between space motions and X-ray luminosity; in Fig. 6 I show X-ray luminosity vs. U and V space motion as an X-ray "bubblegram" with Eggen's (1969) "Young Disk" box; note that one X-ray detected star with very large space motions, i.e., Gl 451 A, is not plotted in Fig. 6. Figure 6 shows that indeed many, albeit not all, X-ray luminous stars are contained in

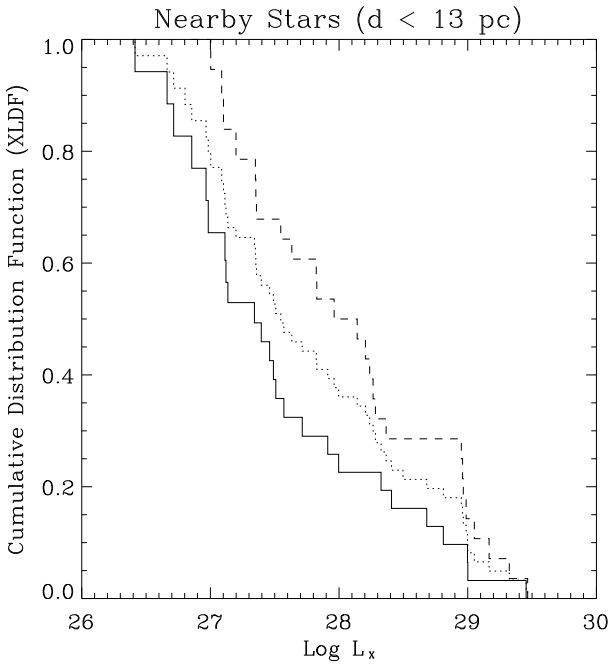

Fig. 5. Cumulative X-ray luminosity distribution functions F-type stars contained in our 13 pc sample (dashed stepped curve), the G-type stars (solid stepped curve), and the full sample (dotted stepped curve).

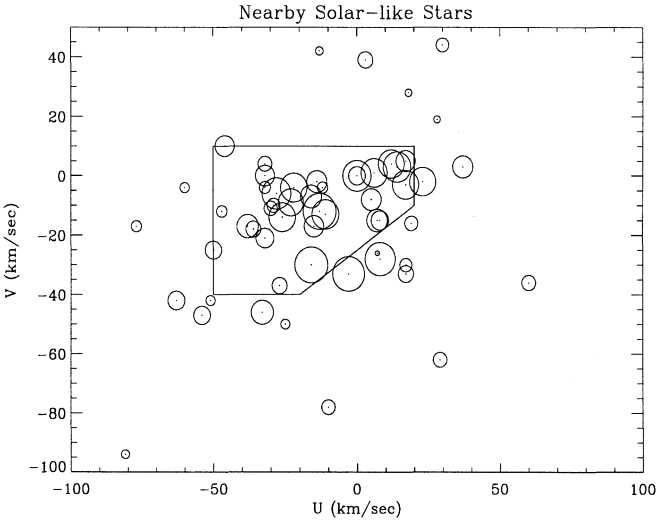

Fig. 6. X-ray luminosity "bubblegram", showing X-ray luminosity (represented by the radius of the symbols plotted) vs. space velocity components of our sample stars; Eggen's (1969) box indicating the space velocity of a young disk population is shown.

"Eggen's box", while stars with lower X-ray luminosity have much less concentrated space motions. A statistical analysis rejects the null hypothesis, that stars within and outside "Eggen's box" have the same X-ray luminosity distribution functions with very high confidence. Thus, I conclude that for the more massive nearby F and G stars kinematic class does provide a reasonable activity indicator.

4.7. X-ray luminosity and spectral hardness

Schmitt et al. (1995) reported a correlation between observed ROSAT PSPC spectral hardness and total X-ray output measured in terms of X-ray luminosity. It is natural to ask to what extent such a correlation is also present for the more massive stars considered in this paper. As in Schmitt et al. (1995), most of the F and G star observations were geared towards source detections only; this particularly applies to the RASS data as well as the follow-up observations of stars not detected in the RASS data. I therefore characterize the spectral properties of the X-ray emission by the measured PSPC hardness ratios (cf., col. 8 in Table 1 and Sect. 3.1). Also, in order to be able to compare different groups of stars I use X-ray surface fluxes instead of X-ray luminosities as activity indicator; stellar radii were computed from the Barnes-Evans relation (Barnes & Evans 1976) using the measured B-V colors, apparent magnitudes and distances. In Fig. 7 I plot X-ray surface flux F_X vs. spectral hardness HR for the X-ray detected sample stars (diamonds); for comparison I also plot the nearby K and M stars (shown in triangles) discussed by Schmitt et al. (1995). The clustering of points at $HR = -1$ is due to data points with low signal-to-noise, where only a signal in the soft PSPC band could be significantly detected; for clarity, the F and G stars have been slightly offset from the later type dwarfs. As is clear from Fig. 7, just like nearby K and dwarfs, the F and G dwarfs populate the hardness ratio range between $-1 < HR < 0$, and increasing X-ray surface flux is correlated with increasing hardness, which in turn implies an increase in the emission measure weighted temperature (cf., discussion by Schmitt et al. 1995). To summarize, I conclude that with respect to the correlation between surface flux and spectral hardness, all late-type dwarf stars behave in the same fashion. In this context it appears worthwhile to point out that studies trying to relate the spectral properties of coronal X-ray emission with its intensity have also been carried out with data from the *Einstein Observatory* (cf., Vaiana 1983; Schmitt et al. 1990); however, these studies had to characterize the observed stellar pulse height spectra parametrically (through fitted coronal temperatures), which very quickly leads to ambiguities in the permissible temperature distributions once more complicated emission measure distributions are allowed.

A salient but interesting feature of Fig. 7 is the fact that apparently no surface fluxes significantly below $F_X \approx 10^4$ erg/cm^2/sec were measured. In order to explore this further I plot in Fig. 8 the surface fluxes vs. $B - V$ color for all of the sample stars of this paper (rather than only the detections) as well as the K and M dwarf sample studied by Schmitt et al. (1995). Figure 8 shows that the apparent cutoff at surface fluxes of $F_{lim} \approx 10^4$ erg/cm^2/sec is not a question of lacking sensitivity. The non-detected A-type stars do indeed have upper limits below F_{lim}, but because of the completeness of the samples both for the F and G stars as well as the K and M stars, I can state that among cool dwarfs stars with X-ray surface fluxes below F_{lim} do not exist (in the considered volumes of space). The star with the lowest **detected** surface flux is the G star Gl

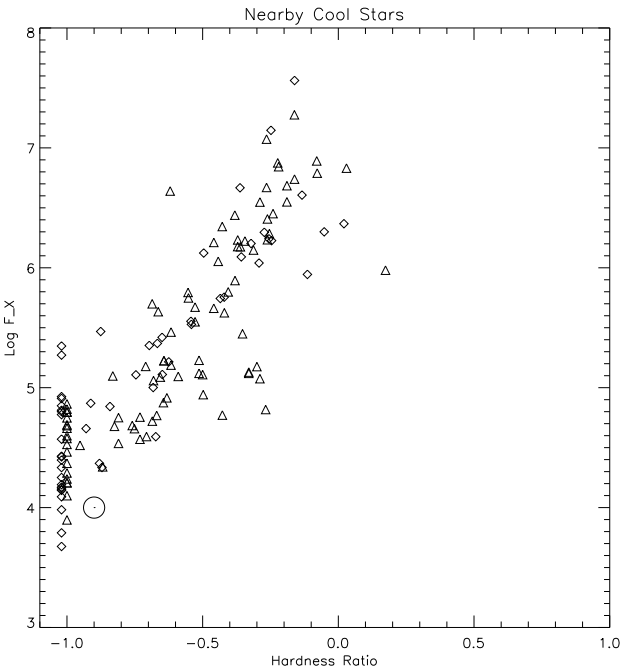

Fig. 7. Plot of X-ray luminosity L_X vs. spectral hardness between soft and hard PSPC counts for F and G stars (diamonds) and K and M stars (triangles; from Schmitt et al. 1995). The correlation between hardness and total X-ray output is obvious, but a large scatter around the regression curve is also apparent. A typical value in terms of F_X and HR for a solar coronal hole is also shown.

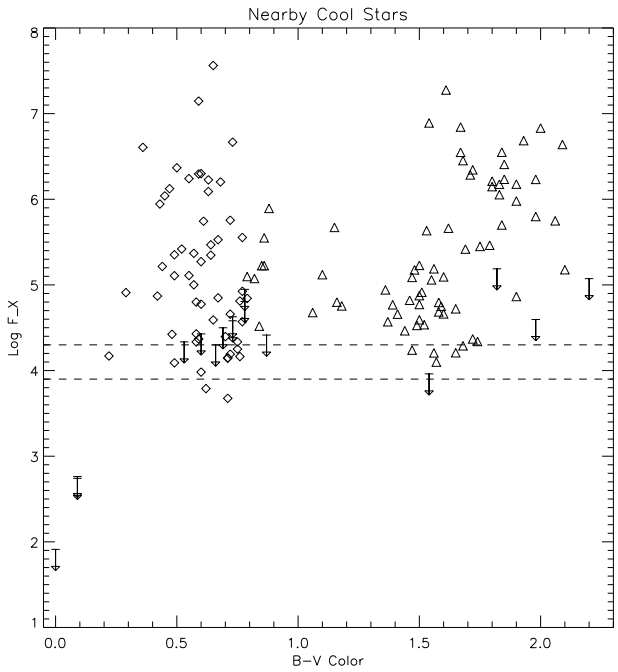

Fig. 8. Mean X-ray surface brightness F_X vs. $B-V$ color for my sample stars (including A-type stars drawn as upper limits). F and G stype stars are plotted with diamonds, K and M type stars (as discussed by Schmitt et al. 1995) with upward triangles. For comparison the typical X-ray surface flux level (in the PSPC band pass) from solar coronal holes is shown by the two dashed curves. Clearly the observed solar coronal hole surface flux provides a good description of the observed stellar minimum X-ray flux. See text for details.

512.1, which was barely detected as a very soft source in a 3 ksec PSPC pointing; this star incidentally is 70 Vir, recently proposed to be surrounded by a planetary companion (Marcy & Butler 1996). The minimum flux maybe slightly increasing with color, i.e., towards redder stars, which have larger surface gravities. Hence, if anything, the minimum flux will increase rather than decrease with surface gravity.

5. Interpretation and conclusions

5.1. Universality of stellar coronae

As is clear from Table 2 and Fig. 3, for stars classified as late A-type or F-type, the detection rate is complete, for stars classified as G-type, the detection rate is very large. I argue that also for the latter group of stars it is reasonable to assume the existence of coronae, since, first, all cases where survey non-detections were reobserved in the pointing program resulted in detections, and second, my upper limits lie well above the lowest detections. The conclusion then is that coronal formation and X-ray emission are universal for stars in the spectral range A7 to G9. Combining this with the findings obtained by Schmitt et al. (1995) it follows that **all** cool dwarf stars must be surrounded by X-ray emitting coronae. The existence of truly X-ray dark cool dwarf stars can of course not be entirely excluded, but one can state with confidence that such objects must be very rare. On the other hand, for nearby A-type stars, specifically the prototypical A-star Vega, extremely sensitive upper limits are now available, which demonstrate that coronae around those stars (if at all existent) must be very different from those around cooler stars.

5.2. The Sun in perspective

With my complete sample of solar-like stars I am now in a position to carry out a fair comparison between solar and stellar X-ray emission. Interestingly, the median of the observed X-ray luminosity distribution function at $log\ L_X = 27.5$ lies actually somewhat above typical solar maximum emission levels. Therefore one must look at the Sun as a star with an activity below average, however, the observed range (between maximum and minimum) of solar soft X-ray luminosity compares well with the low luminosity part of the observed stellar X-ray luminosity distribution function, and therefore the Sun is certainly not atypical among solar-like stars. The X-ray luminosities (cf., Fig. 3 and Fig. 3 in Schmtt et al. 1995) and mean X-ray surface fluxes (cf., Fig. 8) are very similar for the whole sample studied, and in fact for all cool stars when the F and G type dwarfs discussed in this paper are combined with the K and M dwarfs presented by Schmitt et al. (1995). The distribution functions for X-ray luminosity (cf., Fig. 4 and 5, and Fig. 4 in Schmitt et al. 1995) and X-ray surface flux vary smoothly over the observed range of data values with no sign of any bimodal distribution. The most natural explanation for these findings seems to be to assume

Table 4. Ratio of excess to basal flux for minimum flux coronae

Line	B-V = 0.3	B-V = 0.6	B-V = 1.0	B-V = 1.5
SiII	0.25	1.79	25	97
CII	1.73	43	824	1460
SiIV	2.73	55	547	3650
CIV	0.50	9.9	496	2650

that the same heating processes that are operating in the solar corona are also operating in stellar coronae.

5.3. Minimum X-ray surface flux

There appears to be a rather well defined minimum X-ray surface flux below which the observed stellar X-ray emission never drops (cf., Fig. 8); this minimum X-ray surface flux is more or less independent of color. I re-emphasize in this context particularly that the lack of cool stars with mean X-ray surface fluxes below $\approx 10^4$ erg/cm^2/sec is not a selection effect but real; unlike sensitivity-limited studies no clustering of sources near the sensitivity limit is observed.

It is instructive to relate the here derived minimum X-ray flux for solar-like stars to the "basal" heating claimed by the Utrecht group and collaborators to be operating in the atmospheres of cool stars; for a recent review of basal heating cf., Schrijver (1995) and references therein. When different activity indicators such as broad band soft X-ray emission, CIV, CII, Si IV and Si II emission are considered, one generally finds a correlation of these quantities such that stars with the largest X-ray outputs also tend to have the largest outputs in the other activity indicators. When specifically doubly logarithmic regression analyses of flux-flux correlations are considered, Schrijver (1987) found that the scatter around the regression curves is somewhat reduced if a color-dependent arbitrary function is subtracted from each of the activity indicators, and the regression is performed with the excess fluxes (instead of the observed fluxes); for example, Rutten et al. (1991; Table 4) quote fit improvements between 0% (for Si IV vs. Si II) and 64 % (for X-ray vs. Ca II) between the different regression analyses. The arbitrary function, which perhaps not too surprisingly lies close to the minimum observed fluxes, is then called a "basal" flux and interpreted as the result of acoustic heating, while the "excess" flux is attributed to a magnetic heating component.

Interestingly, for the X-ray emission Rutten *et al.* do not require such a basal flux component, or putting it differently, all the X-ray emission has to be considered as an "excess" flux. Having found a minimum X-ray flux, which is interpreted as "excess flux" in the basal picture, one can calculate the "minimum" excess fluxes from the regression fit parameters presented by Rutten et al. (1991) and compare those to the basal fluxes in the various activity indicators. In Table 4 I present the result of this calculation for the C and Si lines and a number of representative B-V colors. As is clear from Table 4, these "minimum excess fluxes" do exceed the basal fluxes for the G, K and M-type stars by factors of up to ten or orders of magnitude. Therefore for those stars the existence of a basal flux or the lack thereof seems to be of little practical relevance. The situation may be somewhat different for the F-type stars, which tend to have the largest basal fluxes in all activity indicators. For $B-V$ = 0.3, the basal fluxes quoted by Schrijver (1995) exceed the "minimum excess fluxes" by factors of 2 and 4 in the CIV and SiII lines respectively. Hence some authors have argued (cf., Mullan & Cheng 1994) that the X-ray fluxes observed especially for early F-type and late A-type stars are basal, with the implication that the underlying heating is acoustic other theoretical arguments notwithstanding. Observationally such an hypothesis cannot be rejected, however, in my opinion none of the observations suggest that the coronal properties of late A-type/early F-type are any different from those of later type stars. The X-ray surface fluxes appear similar (cf., Fig. 8) as well as the spectral distribution of the X-ray emission as far as we can tell from the available PSPC spectra. In addition to the apparent similarity of the X-ray spectra, Schmitt et al. (1996) find - for Procyon - coronal densities consistent with solar active region densities, which strongly argues against the presence of acoustic heating in the corona of that star. As to somewhat cooler atmospheric regions, Walter et al. (1995) studied the CII emission from two late A-type stars, Altair (B-V = 0.22, d = 5 pc, included in our sample) and α Cep (B-V = 0.22, d = 14.7 pc, not included in our sample). Both stars have X-ray surface fluxes near $F_{X,lim}$, yet Walter et al. (1995) conclude that the observed CII emission exceeds the basal fluxes by some factors even for stars as early as $B-V$ = 0.22. Thus the quest for a purely "basal star", conforming to the acoustic heating picture, has been rather elusive. Such stars are surely not impossible by the laws of physics, but nature need not realize all its options and basal stars may well be a chimaera that nature simply does not provide.

5.4. The meaning of the observed minimum flux

All of observed facts suggest that the corona of the Sun and the coronae of other solar-like stars have common heating mechanisms. By appealing to the solar analogy and the observed similarities between the X-ray properties of low-luminosity solar-like stars and the Sun I argue that this heating ought be magnetic rather than acoustic. This is of course in line with theoretical estimates of acoustic heating; Stepień & Ulmschneider (1989) derived an upper bound of ≈ 30 erg/cm^2/sec for solar-like stars as considered in this paper, i.e., a value more than two orders of magnitude below the lowest observed mean surface X-ray flux. If not acoustic, what is then the meaning of the observed minimum flux ?

It is of some interest in this context to consider the minimum X-ray surface fluxes observed for different structural features found in the solar corona. The X-ray emission from the solar corona is characterized by its enormous degree of spatial inhomogeneity as recently exemplified by many thousands of high spatial resolution images taken by the *YOHKOH* satellite. Clearly, the regions with the lowest X-ray fluxes are coronal holes. While such regions often appear black in color

representations of solar X-ray images, the actual X-ray intensity recorded from such regions is non-zero. A variety of techniques has been employed to measure temperature and densities of the coronal hole plasma (cf., Table 1 in Hara et al. 1994). The most precise temperature measurements appear to be those utilizing UV/EUV lines which typically yield temperatures of $\approx 1.5 \times 10^6$ K, on the other hand, the best emission measure measurements appear to be those utilizing soft X-ray images, an approach taken by Maxson & Vaiana (1977), who performed a detailed analysis of *Skylab* observations of coronal holes, and similarly by Hara et al. (1994), who used the *YOHKOH* soft X-ray telescope to derive temperature and emission measure of coronal holes. The latter approach is somewhat hampered by the fact that plasma temperatures are not that well constrained by the rather broad band soft X-ray imaging data; furthermore, extreme care has to be taken in correctly accounting for flux scattered into the wings of the instrumental point response function, because otherwise the coronal hole emission measure will be overestimated. Hara et al. (1994) conclude that the model which best describes all the available observations is a two-temperature model with $T_1 = 1 \times 10^6$ K and $EM_1 = 10^{25.7-25.8}$ cm^{-5} and $T_2 = 2 \times 10^6$ K and $EM_1 = 10^{25.8-25.9}$ cm^{-5}, while Maxson & Vaiana (1977) use a one-temperature model and find that emission measure values between $EM = 10^{25.2-26.3}$ cm^{-5} are consistent with the data depending on which temperature in the range between $T = 1 - 3 \times 10^6$ K is chosen. For the various models consistent with the *Skylab* data (cf., Maxson & Vaiana 1977, their Fig. 10) and the *YOHKOH* data (cf., Hara et al. 1994, their Fig. 6) I have computed the energy fluxes emitted in the 0.1 - 2.4 keV, i.e., the PSPC, pass band. The results of these calculations are shown in Fig. 9, where I plot the X-ray surface flux in the 0.1 - 2.4 keV pass band vs. emission measure; the dotted curve refers to the *Skylab* data and EM is the emission measure of the single temperature component, the solid and dashed lines refer to the *YOHKOH* data and EM denotes the emission measure of the low-temperature component assumed by Hara et al. (1994) to be 1×10^6 K (solid line) and 1.5×10^6 K (dashed line). The upward arrow in Fig. 9 indicates the surface flux corresponding to a coronal hole (single) temperature of 1.3×10^6 K. From Fig. 9 I conclude that the coronal holes studied with *Skylab* and *YOHKOH* produced X-ray surface fluxes between $1 - 2 \times 10^4$ erg/cm^2/sec in the PSPC band pass; smaller surface fluxes can only be achieved if the mean coronal hole temperatures are assumed to be 2×10^6 K or more, which appears to be inconsistent with other data.

The same surface flux range as derived for solar coronal holes is also indicated – by dashed lines – in Fig. 8. Clearly, the observed minimum fluxes for solar-like stars are rather close to the X-ray surface fluxes observed from solar coronal holes. Similarly, in Fig. 7 I also plotted a typical data value for a solar coronal hole, using $F_X = 10^4$ erg/cm^2/sec and assuming a temperature of $1.3\ 10^6$ K, with the HR-temperature conversion from Haisch et al. (1992); obviously, solar coronal holes would appear as extremely soft X-ray sources when observed with the ROSAT PSPC. These observational findings can be interpreted either to be coincidental or alternatively to suggest – again by employing the solar analogy – that the minimum X-ray flux stars are the ones whose total X-ray luminosity is dominated by coronal holes, whereas the more X-ray luminous stars should have significant contributions from either the stellar analogs of quiet Sun large scale structure or active regions or both. If this latter suggestion is correct, one expects mean surface flux and mean coronal density to be correlated. If it is the case that the lower X-ray surface flux envelope of stars with $F_X \sim 10^4$ erg/cm^2/sec are stars completely covered by coronal holes, and the upper X-ray surface flux envelope of stars with $F_X \sim 10^8$ erg/cm^2/sec are stars completely covered by active regions, the mean coronal density should increase by two orders of magnitude from $\approx 10^8$ cm^{-3} to $\approx 10^{10}$ cm^{-3}. The lower density limit is not expected to significantly depend on stellar parameters, while the maximum densities will be higher if the emission scale length drops below the pressure scale height. At present there are unfortunately only a few coronal density measurements for the quiescent emission from solar neighborhood stars available. For the low activity F-star Procyon (cf., Schmitt et al. 1996b) and for the intermediate activity K-star ϵ Eri (cf., Schmitt et al. 1996a) coronal densities with substantial measurement errors but consistent with solar active region densities have been determined; for the active RS CVn like system Capella, Dupree et al. (1993) determine coronal densities from Fe XXI lines in excess of 10^{11} cm^{-3}, and therefore the existing data are certainly not in conflict with the idea that more active coronae are characterized by significantly larger coronal densities.

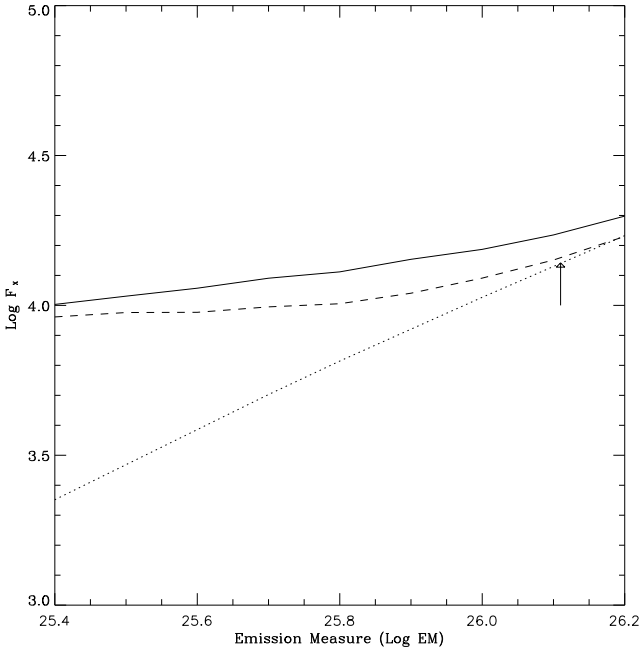

Fig. 9. X-ray surface flux F_X (in the 0.1 - 2.4 keV band) vs. emission measure EM. The dotted curve refers to the *Skylab* data (Maxson & Vaiana 1977), where EM denotes the total emission measure, the solid and dashed lines to *YOHKOH* data (Hara et al. 1994), where EM denotes the emission measure in the lower temperature component assumed at $1\ 10^6$ K (solid curve) and $1.5\ 10^6$ K (dashed curve). See text for details.

5.5. Stellar Maunder minima

The physical properties of the solar atmosphere during the so-called Maunder minimum, i.e., a prolonged state of low or absent activity, have become a subject of considerable scientific interest, ever since Eddy (1976) pointed out in a very convincing fashion that the low sunspot numbers recorded in the period between about 1645 and 1715 should be considered real and not be due to sparse and unreliable observational material. The connection to the Earth's climate was made when variations in the solar output were shown to be related to the solar cycle (Hudson 1988), such that solar maximum activity also corresponds to maximum irradiance. The obvious question then to ask is how typical are Maunder minimum-like episodes for the Sun ?

One approach to answer this question in the context of the solar-stellar connection is to search for Maunder minimum candidates in a sample of solar-like stars. Baliunas & Jastrow (1990) studied the frequency distribution of the mean calcium index $< S >$ of stars contained in the Mount Wilson HK monitoring project (cf., Baliunas et al. 1995); the observed range in this mean index is $0.12 << S >< 0.21$, typical solar values are between 0.164 and 0.178. Baliunas & Jastrow (1990) found a bimodal frequency distribution in $< S >$ with a low-activity peak well separated from solar minimum values. This low-activity peak contains about a third of their sample stars and hence these authors conclude that the "Sun has spent about one-third of its time in the past in several millenia in magnetic minima"; they further suggest that the similar appearance of the Sun in terms of mean sunspot numbers during solar minimum and Maunder minimum "has led to incorrect conclusions about the properties of the Sun in a Maunder minimum" and argue "that the level of magnetic activity is much lower in a Maunder minimum than in a sunspot minimum".

I have investigated the X-ray properties of the stars contained both in my 13 pc sample and in the Mount Wilson HK project; Baliunas et al. (1995) do point out that their sample is not complete with regard to magnitude and distance. Unfortunately only 15 stars are contained in both samples and the median X-ray luminosity of this subsample exceeds the median of the full sample by about a factor of ~ 2. From the X-ray point of view it is extremely unlikely that up to a third of the solar-like stars are in Maunder minimum-like lulls of activity; the lowest third of the X-ray luminosity distribution function contains stars emitting at solar maximum levels ! Further, in the whole sample not a single star does drop significantly below the observed solar-minimum X-ray surface flux. In consequence, Maunder minimum stars must either be quite rare or they cannot differ significantly from the Sun observed at solar minimum. It would obviously be of interest to establish the cycle properties of stars which are known to have very low X-ray surface flux. Some care ought to be exercised in interpreting the statistical results from the Mount Wilson sample; I suspect that this sample is actually somewhat biased, and it would in my opinion be extremely important to study the $< S >$ index distribution in a truly complete sample.

5.6. The big picture

I conclude with a few somewhat more speculative considerations. The new ROSAT observations have shown that all cool stars in the solar neighborhood are X-ray sources with a minimum X-ray surface flux typical for solar coronal holes. The question is whether one attaches physical meaning to this finding or not. To me it seems natural to go for the former, although admittedly it is unclear whether coronal holes on the Sun do indeed have a "minimum flux" or not. Interestingly, also the largest surface fluxes observed for stars are close to the typical radiative loss values observed for solar active regions $\approx 5\ 10^6$ erg/cm^2/sec; cf., Withbroe & Noyes 1977), with only a few stars exceeding this limit. It is therefore suggestive to interpret the observed stellar variety in terms of the coronal features observed on the Sun, i.e., coronal holes, large scale ("quiet") structure, active regions, and a hot component, which is observed on the Sun only during flares. The differences from star to star arise from the filling factors of the various components. In this picture, the observed minimum (I purposely avoid the word "basal" !) flux would be due to emission from magnetically open regions, and cool (main sequence) stars without magnetic fields do – in this picture – simply not exist at least in the observable universe. I would therefore also take issue with the alleged acoustic origin of the "basal" fluxes discussed by Schrijver (1995) in the sense that it is exceedingly difficult to find stars where the "basal" fluxes provide the dominant component; at least at transition region and coronal levels the non-"basal" fluxes exceed the "basal" ones by at least some factors. I emphasize that I am not arguing that such "basal" stars are not possible by the laws of physics, rather I am arguing that nature does not provide such stars very often and not at all within 13 pc around the Sun.

As one goes from "minimum" stars to more and more active stars, more and more of the magnetic topology becomes closed, leading to larger and larger radiative losses from large scale structures and active regions. For the most active stars soft X-ray observations clearly require a hot corona component with a temperature of $\approx 10^7$ K, which provides the bulk of the observed soft X-ray emission measure (cf., Schmitt et al. 1990). This hot component is not present in the solar corona at least under "quiescent" conditions; it is present during solar flares but always in transient from. In the stellar context, such a hot corona component is always present and seems – somehow – to be associated with the production of relativistic particles, which lose energy via gyrosynchrotron radiation as observed at radio wavelengths leading to the correlation between X-ray and radio luminosity for such active stars (cf., Güdel et al. 1993). On the other hand, non-active stars like the Sun (or Procyon for that matter, cf. Drake et al. 1993) are X-ray overluminous with respect to their microwave emission.

My basic ansatz is by no means new. Already Vaiana & Rosner (1978) considered – prior to the launch of the *Einstein Observatory* – how the X-ray output of the Sun would change if the filling factors of its various coronal constituents were changed; in particular they showed that any X-ray luminosity between $\approx 5\ 10^{26}$ erg/sec and $\approx 2\ 10^{31}$ erg/sec can be produced

by going from a coronal hole dominated Sun to a flare dominated Sun. With the ROSAT observations we have the data at hand to demonstrate that nature also realizes the various options.

Acknowledgements. The ROSAT project has been supported by the Bundesministerium für Bildung, Wissenschaft, Forschung und Technologie (BMBF) and the Max-Planck-Gesellschaft (MPG). The continued support for this project by my colleagues from the MPE ROSAT team is gratefully acknowledged. This research has also made use of the Simbad database, operated at CDS, Strasbourg, France. I acknowledge discussions with H. Hudson on solar coronal holes and with M. Hünsch on minimum fluxes, and the help of Prof. Dr. J. Trümper in organizing this paper.

References

Baliunas, S.L., Jastrow, R., 1990, *Nature*, 348, 520
Baliunas, S.L. and 26 authors, 1995, ApJ, **438**, 269.
Barnes, T.G., Evans , D.S., 1976, MNRAS, **174**, 489.
Bopp, B.W., Fekel, F.C., Aufdenberg, J.P., Dempsey, R. Dadonas, V., 1993, AJ **106**, 2502.
Cruddace, R.G., Hasinger, G.R., Schmitt, J.H.M.M., 1988, in *ESO Conf. on Large Astronomical Databases*.28, 77
Drake, S.A., Simon, T., Brown, A., 1993, ApJ, 406, 247.
Dupree, A. K., Brickhouse, N. S., Doschek, G. A., Green, J. C., Raymond, J. C. 1993, ApJ, 418, L41.
Eddy, J.A., 1976, *Science*, **192**, 1189.
Eggen, O.J., 1969, *PASP*, **81**, 553.
Haisch, B., Schmitt, J.H.M.M., Rosso, C., 1992, ApJ Lett **388**, L61.
Golub, L., Harnden, F.R. Jr., Pallavicini, R., Rosner, R., Vaiana, G.S., 1981, ApJ, 253, 242
Grottian, W., 1939, *Naturwiss.*, **27**, 214.
Güdel, M., Schmitt, J.H.M.M., Fleming, T.A., 1993, ApJ, **415**, 236.
Güdel, M., 1994, ApJ Supp, **90**, 743.
Hara, H., Tsuneta, S., Acton, L.W., Bruner, M.E., Lemen, J.R., Ogawara, Y., 1994, PASJ , **46**, 493.
Haisch, B., Schmitt, J.H.M.M., Rosso, C., 1992, ApJ Lett **388**, L61.
Haisch, B., Schmitt, J.H.M.M., Drake, J.J., 1994, ApJ Lett **421**, L39.
Hudson, H.S., 1988, *Ann. Rev. Astron. Astrophys.,* **26**, 473.
Hünsch, M., Schmitt, J.H.M.M., Schröder, K.-P., and Reimers, D., 1996, A&A 310, 801.
Jahreiss, H., 1991, personal communication
Harris, D.E., Johnson, H.M., 1985, ApJ, 294, 649.
Marcy, G.W., Butler, A.P., 1996, ApJ, 464, L147.
Maggio, A., Sciortino, S., Vaiana, G.S., et al., 1987, ApJ **315**, 687.
Maxson, C.W., Vaiana, G.S., 1977, ApJ **215**, 919.
Mullan, D.J., Cheng, Q.J., 1994, ApJ **435**, 435.
Pfeffermann, E., Briel, U.G., Hippmann, H., et al., 1986, SPIE, 733, 519.
Poveda, A., Herrera, M.A., Allen C., Cordero, G., Lavelley, C., 1994, *Rev. Mex. Astron. Astrofis.*, **28**, 43.
Rosner, R., Golub, L., Vaiana, G.S., 1985, *Ann. Rev. Astron. Astrophys.,* **23**, 413.
Rutten, R.G.M., Schrijver, C.J., Lemmens, A.F.P., Zwaan, C., 1991, A&A **219**, 239.
Schmitt, J.H.M.M., Golub, L., Harnden, F.R. Jr., Maxson, C.W., Rosner, R., Vaiana, G.S., 1985, ApJ **290** , 307.
Schmitt, J.H.M.M. and Snowden, S.L., 1990, ApJ **361**, 207.
Schmitt, J.H.M.M., Collura, A., Sciortino, S., Vaiana, G.S., Harnden, F.R., Jr., Rosner, R., 1990, ApJ **365**, 307.
Schmitt, J.H.M.M., Zinnecker, H., Cruddace, R., Harnden, F.R., Jr., 1993, ApJ Lett **402**, L13.
Schmitt J.H.M.M., Güdel, M., Predehl P., 1994, A&A **287**, 843.
Schmitt, J.H.M.M., Fleming, T.A., Giampapa, M.S., 1995, ApJ **450**, 392.
Schmitt, J.H.M.M., Drake., J.J., Haisch, B.M., Stern, R.A., 1996a, ApJ, 457, 882.
Schmitt, J.H.M.M., Drake., J.J., Haisch, B.M., Stern, R.A., 1996b, ApJ, 467, 841.
Schrijver, C.J., 1995, A&A Reviews **6**, 181.
Stepień, K., Ulmschneider, P., 1989, A&A, 216, 139.
Tokovinin, A.A., Shatskii, N.I., 1995, *Astronomy Letters*, **21**, 464.
Trümper, J., 1983, Adv. Space Res., 2, 241
Vaiana, G.S., Rosner, R., 1978, *Ann. Rev. Astron. Astrophys.,* **15**, 363.
Vaiana, G.S., Cassinelli, J.P., Fabbiano, G., et al., 1981, ApJ **245** , 163.
Vaiana, G.S. 1983, in IAU Symposium 102: *Solar and Stellar Magnetic Fields: Origins and Coronal Effects*, ed. J. Stenflo, (Dordrecht: Reidel), 165.
Vaiana, G.S., Maggio, A., Micela, G., Sciortino, S., 1992, *Mem. Soc. Ast. Ita.*, **63** , 545.
Vaiana, G.S. 1983, in IAU Symposium 102: *Solar and Stellar Magnetic Fields: Origins and Coronal Effects*, ed. J. Stenflo, (Dordrecht: Reidel), 165.
Wallerstein, G., Böhm, K.- H., Oke, J.B., 1991, in Extreme Ultraviolet Astronomy, ed. R.F. Malina and S. Bowyer, Pergamon Press.
Walter, F.M., Matthews, L.D., Linsky, J.L., 1995, ApJ **447**, 353.
Withbroe, G.L., Noyes, R.W., 1977, *Ann. Rev. Astron. Astrophys.,* **15**, 363.

This article was processed by the author using Springer-Verlag LaTeX A&A style file *L-AA* version 3.